Available online at www.sciencedirect.com

ScienceDirect

Proceedings of the Combustion Institute 38 (2021) 5403–5414

Proceedings of the Combustion Institute

www.elsevier.com/locate/proci

An a priori assessment of the Partially Stirred Reactor (PaSR) model for MILD combustion

Salvatore Iavarone [a,*], Arthur Péquin [b,c], Zhi X. Chen [a,*], Nguyen Anh Khoa Doan [d], Nedunchezhian Swaminathan [a], Alessandro Parente [b,c,*]

[a] *Department of Engineering, University of Cambridge, Trumpington Street, Cambridge CB2 1PZ, UK*

[b] *Aero-Thermo-Mechanics Laboratory, École Polytechnique de Bruxelles, Université Libre de Bruxelles, Avenue F.D Roosevelt 50, Brussels 1050, Belgium*

[c] *Combustion and Robust Optimization Group (BURN), Université Libre de Bruxelles and Vrije Universiteit Brussel, Bruxelles, Belgium*

[d] *Department of Mechanical Engineering and Institute for Advanced Study, Technical University of Munich, Boltzmannstrasse 15, Garching 85748, Germany*

Received 8 November 2019; accepted 13 June 2020
Available online 2 September 2020

Abstract

Moderate or Intense Low-oxygen Dilution (MILD) combustion has drawn increasing attention as it allows to avoid the thermo-chemical conditions prone to the formation of pollutant species while ensuring high energy efficiency and fuel flexibility. MILD combustion is characterized by a strong competition between turbulent mixing and chemical kinetics so that turbulence-chemistry interactions are naturally strengthened and unsteady phenomena such as local extinction and re-ignition may occur. The underlying physical mechanisms are not fully understood yet and the validation of combustion models featuring enhanced predictive capabilities is required. Within this context, high-fidelity data from Direct Numerical Simulation (DNS) represent a great opportunity for the assessment and the validation of combustion closure formulations. In this study, the performance of the Partially Stirred Reactor (PaSR) combustion model in MILD conditions is *a priori* assessed on Direct Numerical Simulations (DNS) of turbulent combustion of MILD mixtures in a cubical domain. Modeled quantities of interest, such as heat release rate and reaction rates of major and minor species, are compared to the corresponding filtered quantities extracted from the DNS. Different submodels for the key model parameters, i.e., the chemical time scale τ_c and the mixing time scale τ_{mix}, are considered and their influence on the results is evaluated. The results show that the mixing time scale is the leading scale in the investigated cases. The best agreement with the DNS data regarding the prediction of heat release rate and chemical source terms is achieved by the PaSR model that em-

* Corresponding author.
E-mail addresses: si339@cam.ac.uk (S. Iavarone), zc252@cam.ac.uk (Z.X. Chen), alessandro.parente@ulb.be (A. Parente).

https://doi.org/10.1016/j.proci.2020.06.234

ploys a local dynamic approach for the estimation of the mixing time scale. An overestimation of the OH species source terms occurs in limited zones of the computational domain, characterized by low heat release rates.

Keywords: Moderate or Intense Low-oxygen Dilution (MILD) combustion; Partially Stirred Reactor (PaSR); Direct Numerical Simulation (DNS); *A-priori* analysis

1. Introduction

Combustion technologies must undergo a profound innovation in terms of fuel flexibility, pollutant emissions, and thermal efficiency, to provide a clean and affordable solution to the increasing environmental concerns [1]. In the last decades, Moderate and Intense Low-oxygen Dilution (MILD) combustion [2,3] appeared to be a promising technology because of its capability to deliver abated pollutant emissions with elevated thermal efficiency and fuel flexibility. These features are achieved via Exhaust Gases Recirculation (EGR) in the reaction zone. EGR preheats the reactants above their auto-ignition temperature and decreases the oxygen concentration. As a consequence, MILD combustion occurs within distributed reactive zones rather than within a flame front [4] and achieves reduced peak temperatures and pollutants concentrations, which are desirable for industrial applications. Turbulence-chemistry interactions are naturally enhanced in MILD combustion [5] and may lead to unsteady phenomena such as local extinction and re-ignition [6]. In numerical simulations, they also result in additional difficulties in modeling the chemical source term in the species transport equations. The combustion closure in MILD conditions still remains a key issue [7] and has been treated in many different ways, both in Reynolds-Averaged Navier–Stokes (RANS) and Large Eddy Simulation (LES) frameworks. Several numerical studies have employed combustion models like probability density function (PDF) methods [8–10] and Eddy Dissipation Concept (EDC) in both RANS and LES [10–13]. LES investigations with a Perfectly Stirred Reactor (PSR) closure [14] and a flamelet/progress variable (FPV) approach [15] were also carried out. Chomiak [16] proposed the Partially Stirred Reactor (PaSR) model as an alternative to the EDC model, and better results in terms of prediction of temperatures and main species concentrations have been achieved by RANS and LES studies employing different formulations of the PaSR model [17–19]. These models have been validated against experimental data collected in flames and reactors operated in MILD conditions [8,20,21]. More recently, Direct Numerical Simulation (DNS) has become a powerful tool for the assessment and validation of combustion models in MILD conditions [22–24]. Furthermore, by solving the whole turbulence scale spectrum, DNS allows to gather useful insights about the morphology of the MILD reaction zones and their interactions with turbulent structures [5,25] and ultimately to shed light on fundamental processes of MILD combustion such as the absence of visible flames and the presence of strongly convoluted reaction zones [26]. The present study aims to leverage DNS data of turbulent MILD combustion [26] to perform an *a priori* assessment of the Partially Stirred Reactor combustion model as a predictive sub-grid scale (SGS) model for LES. Predictive simulation capabilities are necessary for design and optimization of burners and furnaces operating in the MILD regime. This paper is organized in the following way. The Partially Stirred Reactor is presented in Section 2. The methodology to conduct the DNS is described in Section 3 along with the chemical kinetic mechanism used in this work. Results are presented and discussed in Section 4. Conclusions are summarized in the final section.

2. The Partially Stirred Reactor (PaSR) model

The chemical reaction rates, based on the Arrhenius law, are highly non-linear. Therefore, the mean reaction rates cannot be derived from the average quantities (species mass fractions, density, temperature) in a straightforward way. Turbulent combustion models are then required to provide closure for the chemical source terms in the RANS and LES species transport equations. In the Partially Stirred Reactor (PaSR) model [16], each computational cell is split into two regions: a reacting zone and a non-reacting zone. The mean (or filtered) cell reaction rate $\bar{\dot{\omega}}_i$, which is provided to the species transport equation, is obtained based on a mass exchange between the two regions and expressed as:

$$\bar{\dot{\omega}}_i = \kappa \frac{\bar{\rho}(Y_i^* - Y_i^0)}{\tau^*}, \tag{1}$$

where $\bar{\rho}$ is the Reynolds-averaged density, Y_i^0 and Y_i^* are the ith species mass fractions in the non-reactive region and in the reactive zone, respectively, and τ^* represents the residence time in the reactive structure. The parameter κ is the volume fraction of the reactive zone and thus provides the partially stirred condition. κ is estimated as the ratio between the chemical time scale τ_c and the sum of the chemical time scale and the mixing time scale τ_{mix}, i.e., $\kappa = \tau_c/(\tau_c + \tau_{mix})$ [27]. The sub-grid quantity Y_i^* is obtained by considering the reactive zone as an ideal reactor (either a perfectly stirred reactor or a plug flow reactor) evolving from Y_i^0 during the residence time τ^*. Therefore, the following equation is solved:

$$\frac{dY_i^*}{dt} = \frac{\dot{\omega}_i^*}{\rho}. \tag{2}$$

The term $\dot{\omega}_i^*$ is the instantaneous formation rate of the ith species. The final integration of dY_i^*/dt over the residence time τ^* results in the estimation of Y_i^*. The residence time τ^* is considered to be the mixing time scale [27], and is also the time over which the ideal reactor is integrated, however in other works, including the present study, it equals the minimum between τ_c and τ_{mix} [19,28]. The estimation of chemical and mixing time scales becomes crucial to ensure accurate predictions from the model. Different approaches have been developed to estimate these timescales. As far as the chemical time scale is concerned, Chomiak and Karlsson [29] proposed an estimation based on the formation rates of the species acting as fuel and oxidizer,

$$\frac{1}{\tau_c} = \max\left(\frac{-\dot{\omega}_F}{Y_F}, \frac{-\dot{\omega}_O}{Y_O}\right), \tag{3}$$

where $\dot{\omega}$ is the global conversion rate, Y is the species mass fraction, and the subscripts F and O stand for fuel and oxidizer, respectively. Fuel and oxidizer were deemed to best represent the changes in the reacting system. Fox and Varma [30] suggested estimating the chemical time scale via the calculated eigenvalues of the Jacobian matrix $J_{jk} = \partial\dot{\omega}_j/\partial Y_k$, where $\dot{\omega}_j$ is the jth species net production rate and Y_k the kth species mass fraction. The decomposition of the Jacobian matrix of the species source terms, while allowing to consider complex chemical kinetic schemes, is a time-consuming method for the evaluation of τ_c. As a compromise between accuracy and computational cost, other works [18,19] used the approach based on the species formation rates by considering the slowest chemical time scale as the leading one,

$$\tau_c = \max\left(\frac{Y_i^*}{|\, dY_i^*/dt \,|}\right). \tag{4}$$

As far as the mixing time scale is concerned, Krrholm and Nordin [27,31] estimated it as a certain fraction of the integral time scale τ_{mixI}, related to the eddy break-up time leading from large-scale to Kolmogorov-scale turbulent vortexes,

$$\tau_{mix} = C_{mix}\tau_{mixI} = C_{mix}\frac{k}{\varepsilon}, \tag{5}$$

where k is the turbulent kinetic energy, ε its dissipation rate and C_{mix} the mixing constant, ranging from 0.001 to 0.3. Chomiak and Karlsson [29] proposed a definition based on the geometrical mean of integral and Kolmogorov time scales. The latter is defined as $\tau_{mixK} = \sqrt{\nu/\varepsilon}$, where ν is the kinematic viscosity, and represents the assumption that, in conventional combustion systems, reactions occur at the dissipation scale, of the order of the Kolmogorov one. The geometrical mean of integral and Kolmogorov time scales is then estimated by

$$\tau_{mixMean} = \sqrt{\tau_{mixI}\tau_{mixK}} = \sqrt{\frac{k}{\varepsilon}\left(\frac{\nu}{\varepsilon}\right)^{1/2}}. \tag{6}$$

All the presented submodels for the determination of the turbulent time scale can be regarded as global approaches. A more comprehensive and local definition for τ_{mix} was designed by Senouci et al. [32] and involves the mixture fraction Z. The approach employs the ratio of the mixture fraction variance $\widetilde{Z''^2}$ to the mixture fraction dissipation rate $\tilde{\chi}$,

$$\tau_{mix} = \frac{\widetilde{Z''^2}}{\tilde{\chi}}. \tag{7}$$

The above review clearly indicates that the determination of the characteristic scales is not universal and still subject to discussion, highlighting a lack of generality. To widen the applicability range of the PaSR model, high-fidelity data from DNS represent a great opportunity to evaluate the performances of the PaSR model and improve its predictive capability. In this perspective, an *a priori* assessment of the above-mentioned formulations for both the characteristic timescales τ_c and τ_{mix} is performed by comparing modeled species production/consumption and heat release rates with the corresponding quantities directly filtered from DNS data of MILD combustion. Details about the DNS methodology are given in the following section.

3. Direct Numerical Simulation data

The DNS data of MILD combustion of a mixture of methane, air, and exhaust gases, having spatial and temporal variations of mixture fraction, are used in this study. The turbulence and thermo-chemical conditions of the mixture correspond to the Case AZ1 of Doan et al. [26], and the flow and mass fraction fields for the DNS are generated by the procedure described therein. The turbulence conditions of Case AZ1 are the same as for a premixed reference case studied in earlier

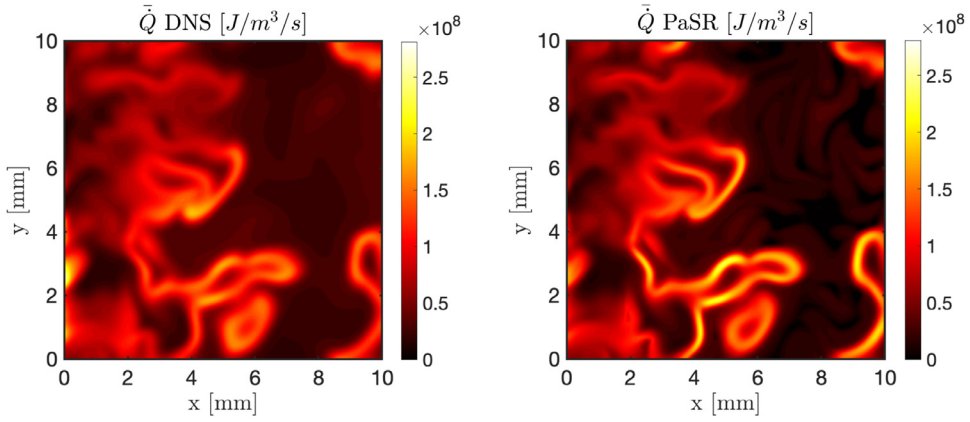

Fig. 1. Filtered heat release rates in the mid x–y plane: (a) extracted from the DNS data; (b) obtained by the PaSR model. The dynamic approach (Eq. (7)) is considered for the evaluation of the mixing time scale τ_{mix}, whereas the formation rate approach (Eq. (4)) is used for the calculation of the chemical time scale τ_c.

works [5,22,25]. Case AZ1 is the non-premixed counterpart of the reference case as it includes a spatio-temporally varying mixture fraction field. The turbulence field has an integral length scale of $\Lambda_0 \approx$ 1.42 mm and a root mean square value of $u' \approx$ 16.66 m/s for the velocity fluctuations. The turbulence and Taylor microscale Reynolds numbers are $\mathrm{Re}_t \approx 96$ and $\mathrm{Re}_\lambda \approx 35$, respectively. The turbulence Reynolds number is similar to those in previous experimental studies of MILD combustion [21,33,34]. Case AZ1 has 3.5% by volume as maximum oxygen concentration. Additional information regarding the mixture fraction and progress variable fields can be found in the Supplemental Material.

The conservation equations for mass, momentum, energy and species mass fractions are solved using the *SENGA2* code [35]. The code has been used in previous studies of MILD combustion, where additional details about the derivative schemes and boundary conditions can be found [5,22,26]. The kinetic mechanism *MS-58* is used for the chemistry and consists of 19 species and 58 reactions [26]. The DNS cubic domain of size $L_x = L_y = L_z = 0.01$ m is discretised using 512^3 uniform grid points which ensures a sufficient resolution ($\delta_x = 20$ μm) for the turbulent and chemical length scales of interest. The simulation was run for 1.5 flow-through time τ_f, defined in [22], before collecting data for statistical analysis. For the present study, the quantities of interest are obtained from the DNS by applying Gaussian filtering and Favre averaging operations [22]. The filter size is $\Delta = 20$ times the DNS grid size and corresponds to a normalised filter size $\Delta^+ = 0.25$, defined as $\Delta^+ = \Delta\delta_x/\delta^m_{th}$, where $\delta^m_{th} = 1.6$ mm is the thermal thickness obtained from the corresponding MILD Flame Element (MIFE) laminar calculation [5] using the mean mixture fraction.

4. Results and discussion

The capability of the PaSR model to predict the filtered heat release rate $\bar{\dot{Q}}$ and filtered species source terms $\bar{\dot{\omega}}_i$ is assessed by considering the filtered quantities in the mid x-y plane of the cubical domain at a time $t = 2\tau_f$. The heat release rate is obtained by $\bar{\dot{Q}} = -\sum_{i=1}^{N_s} \Delta h_i^f \bar{\dot{\omega}}_i$, where Δh_i^f is the enthalpy of formation of the ith species. The filtered species source terms $\bar{\dot{\omega}}_i$ is computed by the PaSR model according to Eq. (1). The chemical time scale is computed via the formation rate approach (Eq. (4)), whereas the mixing time scale is estimated via the dynamic approach (Eq. (7)). The quantities required for the calculation of τ_c and τ_{mix} are taken by filtering the corresponding DNS data. The contours of the heat release rate $\bar{\dot{Q}}$ extracted from the DNS data and estimated by the PaSR model are shown in Fig. 1a and 1b, respectively. Reactions occur over a large portion of the domain in convoluted zones, rather than in a clearly distinguished flame front, as expected. A close agreement between the DNS data and the estimations from the PaSR model can be noticed, particularly in the zones of high rates, where the profiles of the convoluted reaction zones are well captured. The agreement between the species production/consumption rates obtained from the DNS and modeled by PaSR is assessed by looking at the parity plots shown in Fig. 2. The filtered source

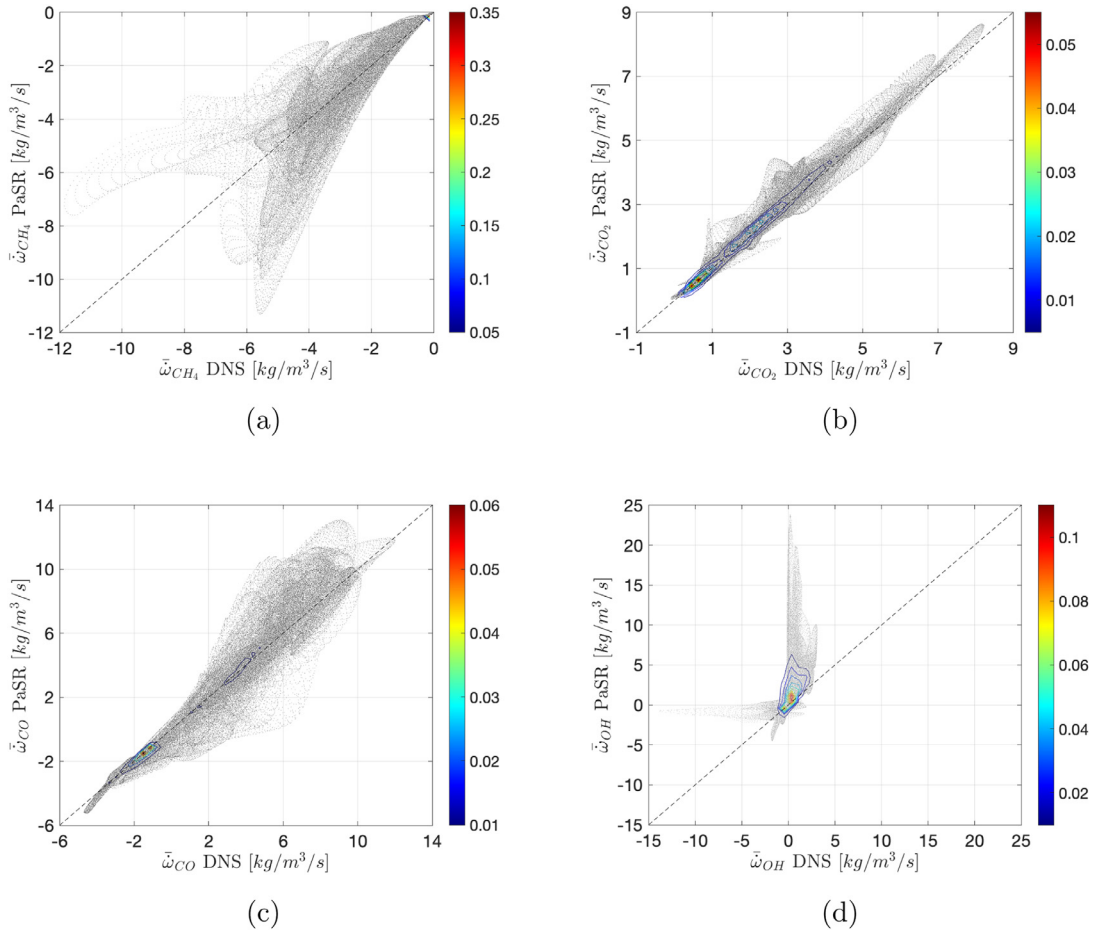

Fig. 2. Parity plots and contours of the joint PDF of the filtered chemical source terms $\bar{\dot{\omega}}$ extracted from DNS and estimated by the PaSR model for: (a) CH_4, (b) CO_2, (c) CO, (d) OH. The dynamic approach (Eq. (7)) is considered for τ_{mix}, whereas the formation rate approach (Eq. (4)) is used for τ_c.

terms of three main species, CH_4, CO_2, and CO, and an intermediate one, OH, are considered. All the grid points of the mid x–y plane are shown in each plot. The contours of the joint PDF of $\bar{\dot{\omega}}_i^{\mathrm{DNS}}$ and $\bar{\dot{\omega}}_i^{\mathrm{PaSR}}$ for the samples collected on the x–y plane are also shown. The PaSR model predicts the source terms of the main species fairly well, while it performs slightly worse in estimating the net production rate of OH, especially for the points of the plane where the DNS rates are close to zero. However, the values that fall far from the $y = x$ line constitute a small fraction of the whole ensemble. This is also true for the CH_4 filtered rates since the great majority of the source term values is concentrated in the upper right corner of Fig. 2a. The contour of the absolute error $\Delta\bar{\dot{\omega}}_{\mathrm{OH}} = \bar{\dot{\omega}}_{\mathrm{OH}}^{\mathrm{PaSR}} - \bar{\dot{\omega}}_{\mathrm{OH}}^{\mathrm{DNS}}$ at the mid x–y plane is shown in Fig. 3a. It can be seen that the highest overestimation of the OH source term occurs in the right region of the plane, where the reactivity is low, as confirmed by the contours of the heat release rates in Fig. 1. The overestimation can be explained by looking at the contour map of the mixing time scale τ_{mix}, shown in Fig. 3b. The zones of high $\bar{\dot{\omega}}_{\mathrm{OH}}^{\mathrm{PaSR}}$ correspond to those where τ_{mix} is extremely small, making the $\kappa\rho/\tau^*$ term of Eq. (1) significantly large. On the other hand, the $(Y_{\mathrm{OH}}^* - Y_{\mathrm{OH}}^0)$ term does not reach low enough values to compensate for the high $\kappa\rho/\tau^*$ term and bring back the PaSR source term close to zero. The mixing time scale is the leading scale for the investigated case, being lower than the chemical time scale all over the mid x–y plane.

To assess the impact of the mixing time scale on the PaSR predictions, a different formulation for τ_{mix} is considered: τ_{mix} is calculated as a fraction of the integral time scale (see Eq. (5)). The constant C_{mix} in Eq. (5) is imposed equal to 0.5, according to Ferrarotti et al. [17]. The parity plots in Fig. 4 show that the PaSR model performs slightly better

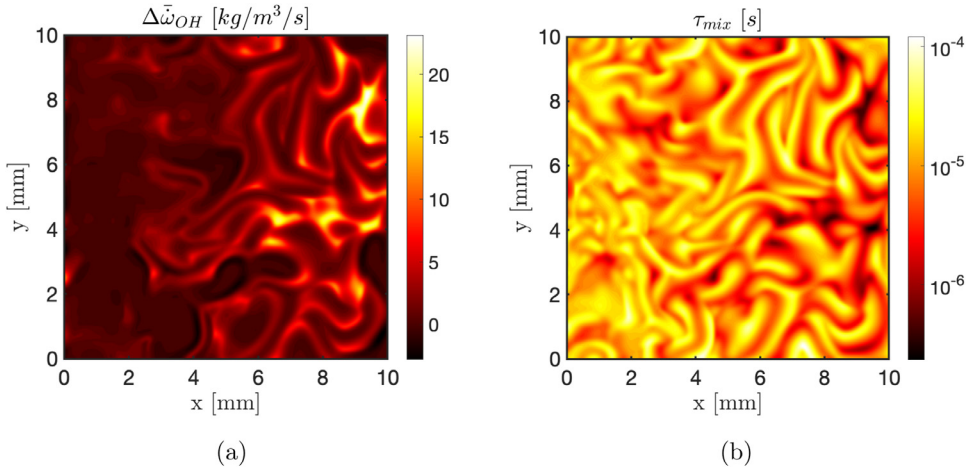

Fig. 3. Filled contour plots of (a) the absolute error between the OH filtered reaction rates from the PaSR model and the DNS, and (b) the mixing time scale τ_{mix} at the mid x–y plane.

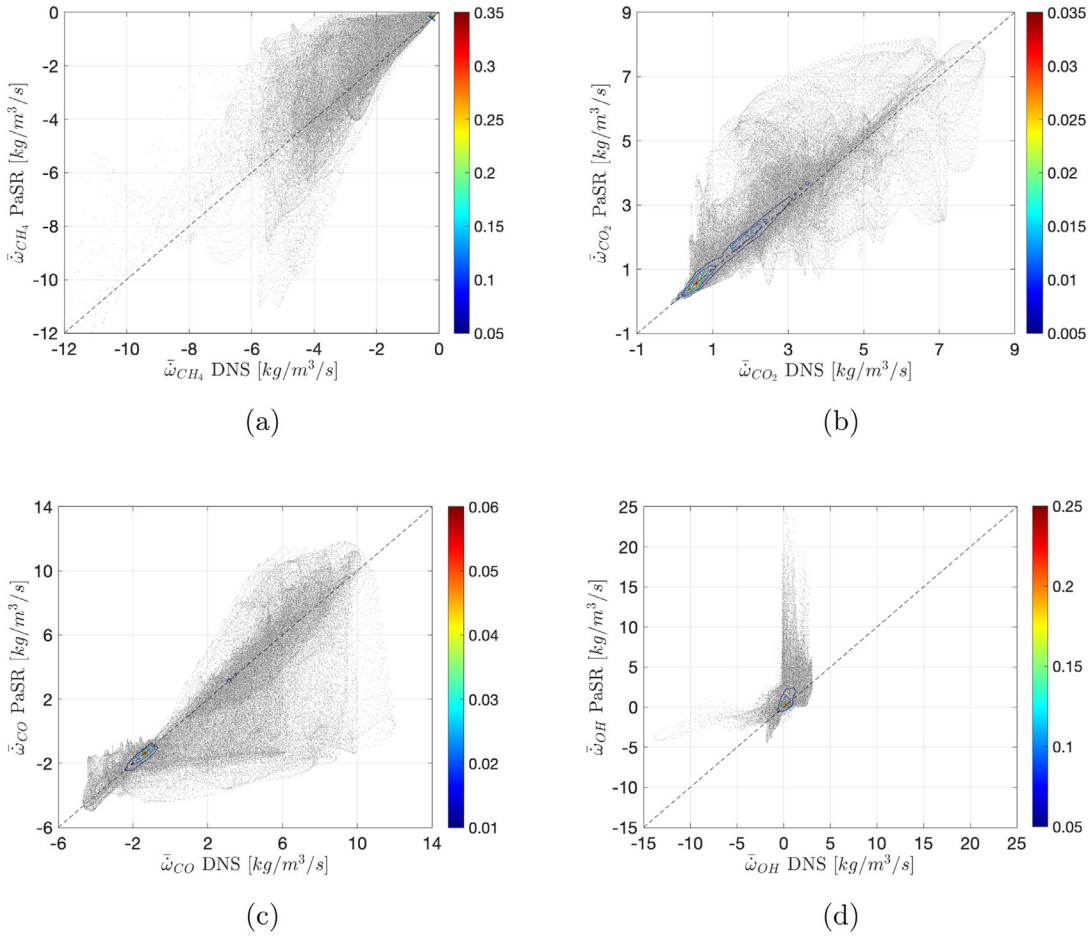

Fig. 4. Parity plots and contours of the joint PDF of the filtered chemical source terms $\bar{\omega}$, extracted from DNS and estimated by the PaSR model, for: (a) CH_4, (b) CO_2, (c) CO, (d) OH. The integral time scale approach (Eq. (5)) is considered for the evaluation of τ_{mix}.

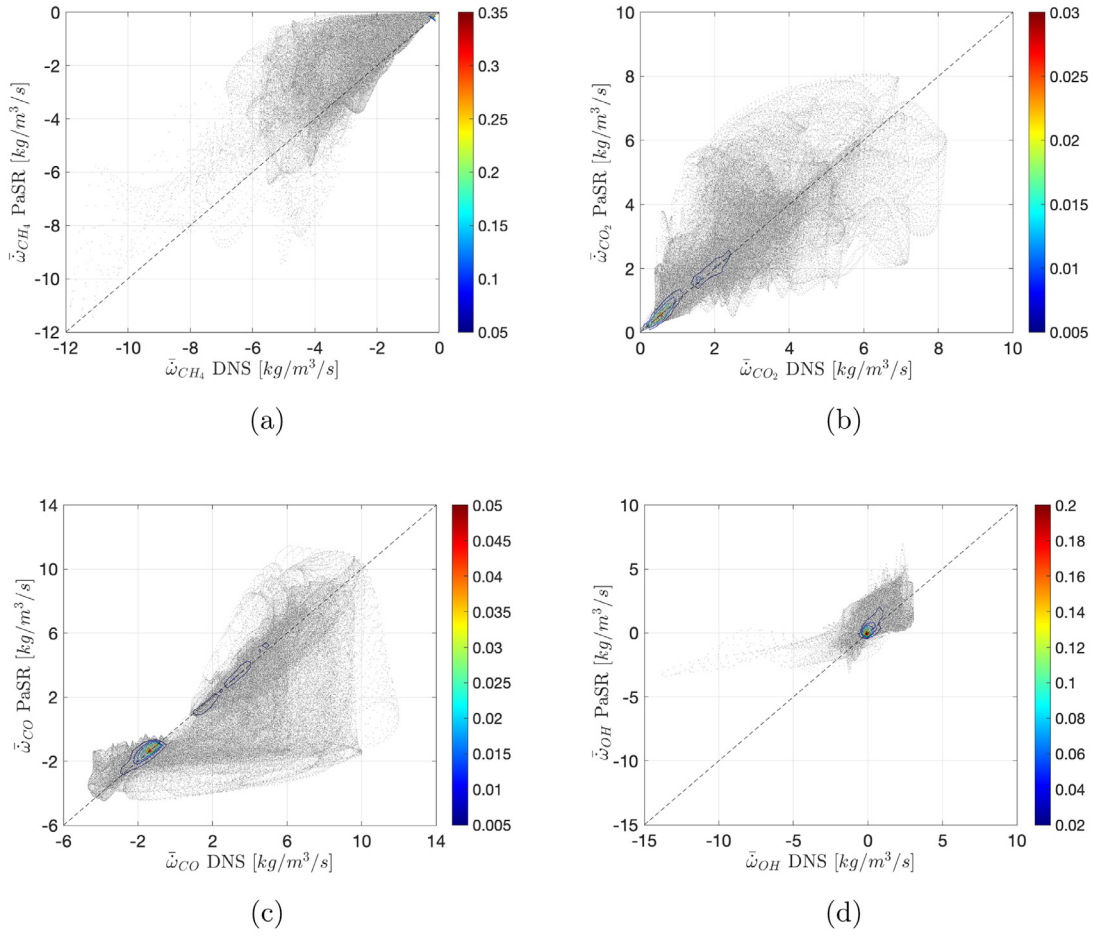

Fig. 5. Parity plots and contours of the joint PDF of the filtered chemical source terms $\bar{\dot{\omega}}$, extracted from DNS and estimated by the PaSR model, for: (a) CH_4, (b) CO_2, (c) CO, (d) OH. The geometrical mean approach (Eq. (6)) is considered for the evaluation of τ_{mix}.

for OH, although a larger scatter of the data across the $y = x$ line is seen for the other species.

A different submodel for τ_{mix} is then considered, namely the approach that estimates τ_{mix} from the geometrical mean of integral and Kolmogorov time scales (see Eq. (6)). The estimation of the filtered OH source term is greatly improved by employing the geometrical mean approach for the mixing time scale, as shown in Fig. 5. However, the source terms of the main species are not affected in the same way by the considered τ_{mix} formulation.

The sensitivity of the results of the PaSR model to the chemical time scale is subsequently assessed. The formulation proposed by Chomiak and Karlsson [29] is considered (see Eq. (3)). According to this approach, the fuel and oxidizer chemical time scales are evaluated and the lowest (fastest) time is used to calculate τ_c and identify the limiting reactant. Although this method follows an opposite rationale compared to the formation rates approach (see Eq. (4)), the impact on the prediction of the source terms is minor for all the species but CO_2, as shown in Fig. 6. This is explained by the fact that the chemical time scale of CO_2 is overall higher than the one of the limiting reactant. Hence, accounting for a faster time scale worsens the prediction of this slow species. The amount of points lying on the $y = x$ lines is reduced for all the species, compared to the corresponding plots in Fig. 2.

A compromise between the formation rate formulation and the approach proposed by Chomiak is to partition the space of chemical time scales into fast/slow subspaces, and to impose τ_c equal to the so-called τ_{M+1} time scale, which corresponds to the fastest of the slow time scales, in accordance with the procedure proposed by Valorani et al. [36]. Figure 7 shows that the predictions of the PaSR model are improved with respect to the previous τ_c formulation and are comparable with the

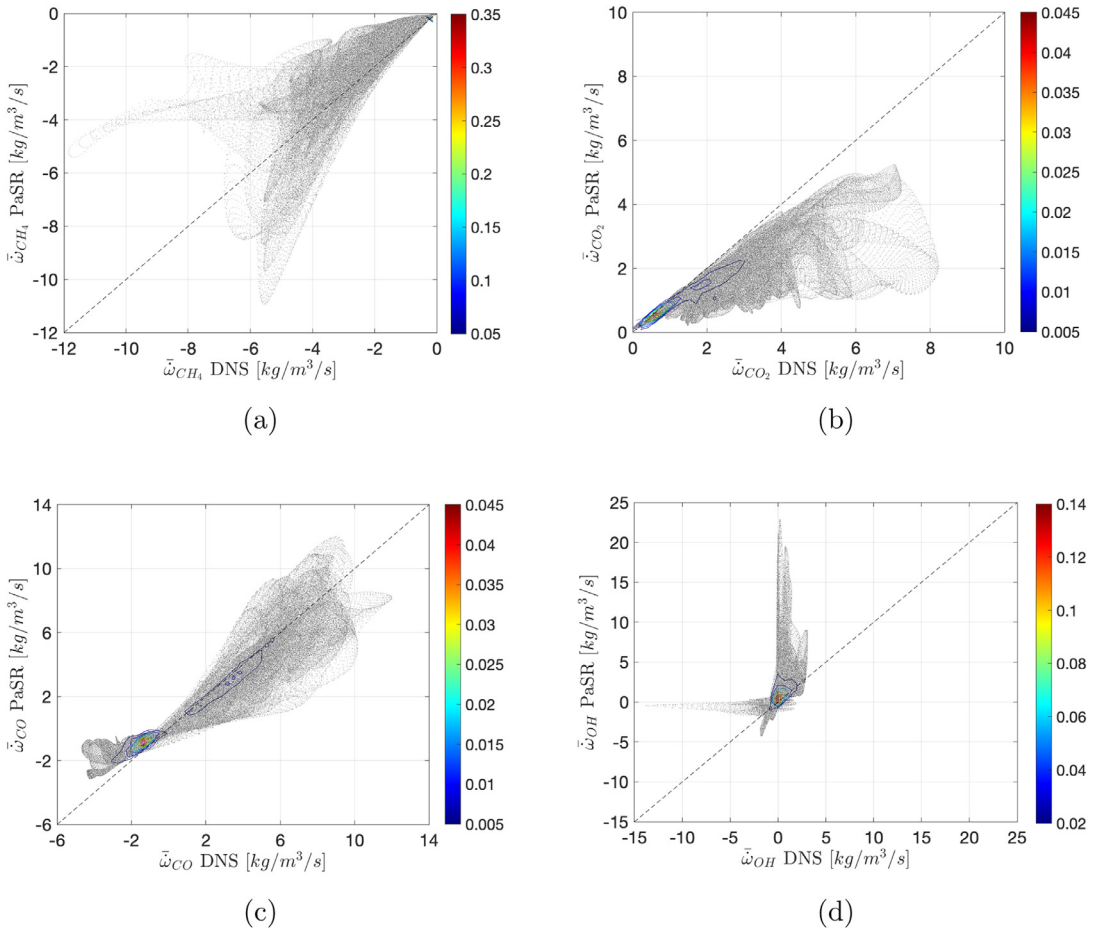

Fig. 6. Parity plots and contours of the joint PDF of the filtered chemical source terms $\bar{\dot{\omega}}$, extracted from DNS and estimated by the PaSR model, for: (a) CH_4, (b) CO_2, (c) CO, (d) OH. The Chomiak approach (Eq. (3)) is considered for the evaluation of the chemical time scale τ_c.

results achieved by the PaSR model employing the dynamic approach for τ_{mix} and the formation rate formulation for τ_c (Fig. 2).

The comparison of the different formulations of the PaSR model has proven that the mixing time scale is the leading scale for the majority of the investigated cases, with $\tau_{mix} << \tau_c$ almost overall for all the PaSR versions but the one that uses the Chomiak formulation for τ_c. The mixing time scale determines the residence time τ^* in Eq. (1) and thus has a considerable impact on the predictions of the filtered chemical source terms. Overall, the best performances are achieved by the PaSR model employing the formation rate approach for τ_c and the dynamic estimation of τ_{mix}, although the source terms for the intermediate OH species are not well captured in the zones of low reactivity, possibly undermining the use of the mixing time of a non-reacting scalar, such as the mixture fraction Z, for the evaluation of τ_{mix}. Moreover, the performance of this PaSR model version declines with larger filter sizes ($\Delta \geq 60$) and this is inherently connected with the magnitude of the dynamic mixing time scale and how it compares with the distributions of the species chemical time scales. The effect of the filter size on the PaSR model predictions is reported in the Supplementary Material.

An additional case, namely case BZ1 of Doan et al. [26], has also been investigated to further validate the performances of the PaSR model that employs the formation rate approach for τ_c and the dynamic formulation for τ_{mix}. Case BZ1 is constructed such that its mixing length is the same as AZ1 but with a higher dilution level. Case BZ1 has a lower maximum concentration of oxygen in the DNS domain, i.e., 2% O_2, and lower stoichiometric and mean mixture fractions with respect to case AZ1. Therefore, case BZ1 is chosen to investigate

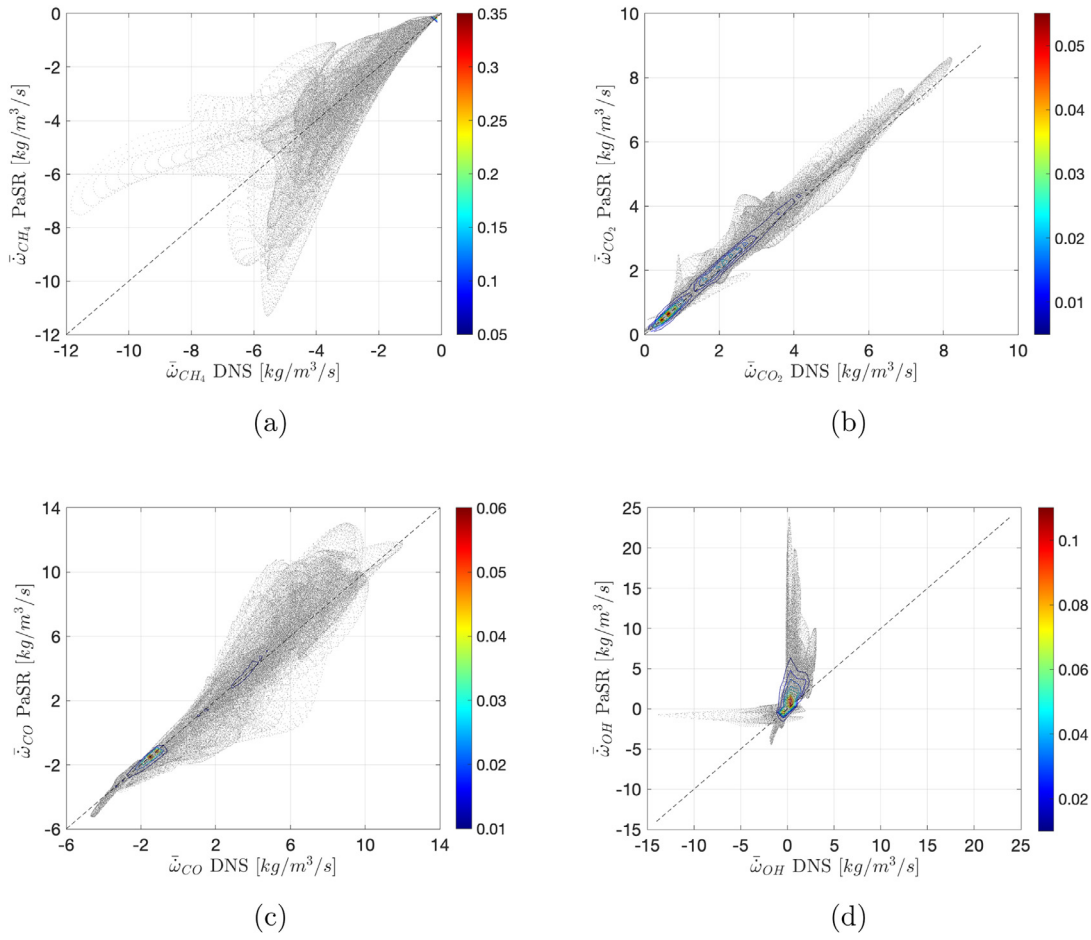

Fig. 7. Parity plots and contours of the joint PDF of the filtered chemical source terms $\bar{\dot{\omega}}$, extracted from DNS and estimated by the PaSR model, for: (a) CH_4, (b) CO_2, (c) CO, (d) OH. The $\tau(m+1)$ approach is considered for the evaluation of τ_c.

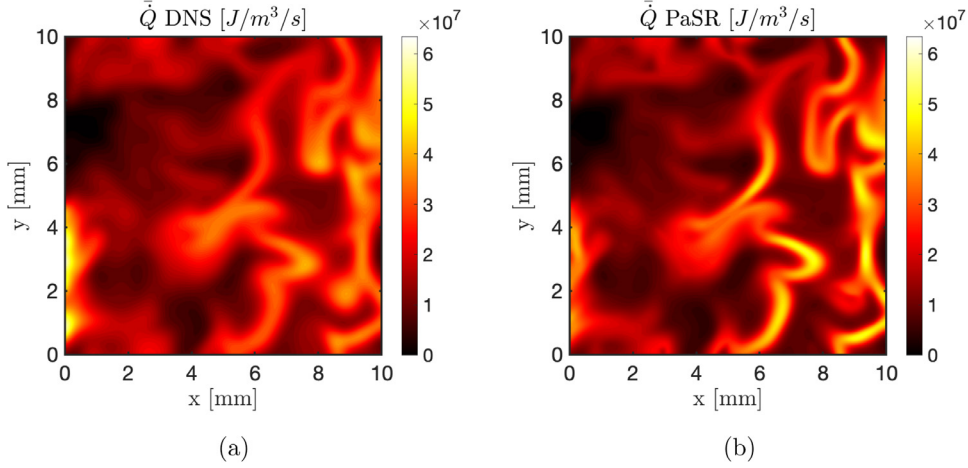

Fig. 8. Filtered heat release rates in the mid x–y plane for case BZ1: (a) extracted from the DNS data; (b) obtained by the PaSR model. The dynamic approach (Eq. (7)) is considered for τ_{mix}, whereas the formation rate approach (Eq. (4)) is used for τ_c.

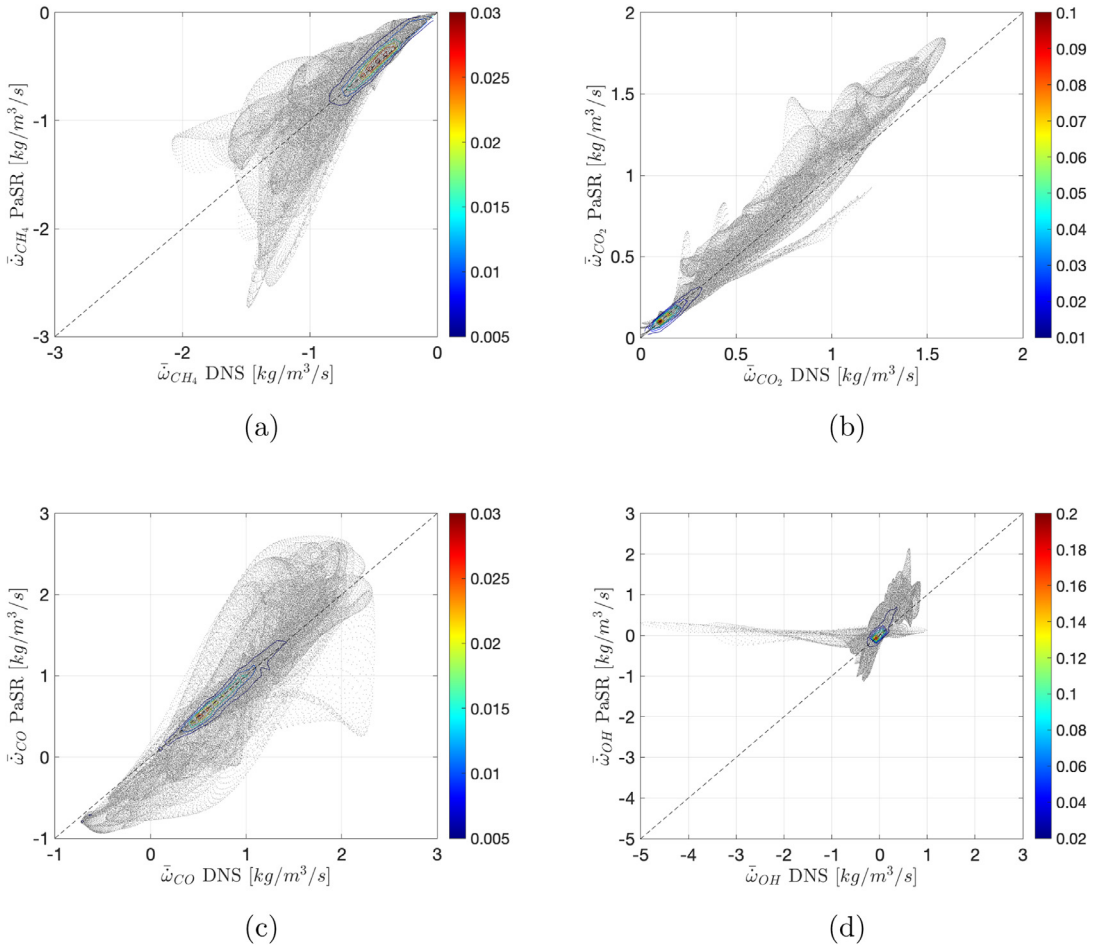

Fig. 9. Parity plots and contours of the joint PDF of the filtered chemical source terms $\bar{\dot{\omega}}$, extracted from DNS and estimated by the PaSR model, for: (a) CH_4, (b) CO_2, (c) CO, (d) OH. The dynamic approach (Eq. (7)) is considered for τ_{mix}, whereas the formation rate approach (Eq. (4)) is used for τ_c.

the dilution effects on the PaSR model performance. The DNS data of case BZ1 are filtered using a Gaussian filter size $\Delta = 30$, corresponding to a normalised filter width $\Delta^+ = 0.25$, same as for case AZ1. The contours of the heat release rate $\bar{\dot{Q}}$ filtered from the DNS and estimated by the PaSR model are shown in Fig. 8a and 8b, respectively. Reactions occur over a larger portion of the domain within thicker and more convoluted zones with respect to case AZ1. These reacting regions are once again well captured by the PaSR model. The filtered DNS species source terms and those obtained by PaSR are shown in the parity plots of Fig. 9. As for case AZ1, the filtered source terms of CH_4, CO_2, CO, and OH, are considered. The PaSR model predicts the source terms of the main species satisfactorily. Moreover, the estimation of the chemical source term of the intermediate species OH is adequate.

5. Conclusions

The predictive capabilities of the Partially Stirred Reactor (PaSR) model in MILD combustion conditions have been *a priori* tested using the DNS filtered heat release rate $\bar{\dot{Q}}$ and species source terms $\bar{\dot{\omega}}_i$. The comparison between the filtered quantities extracted from the DNS data and obtained from the PaSR model shows good agreement for heat release and major species formation/consumption rates, for the turbulence and thermo-chemical conditions considered in this study. The best results are achieved by the PaSR formulation employing the dynamic approach for the mixing time scale and the formation rate estimation for the chemical time scale. For the less diluted case, this PaSR formulation suffers at capturing the filtered source term of the minor species OH in the zones of low reactivity.

Although various characteristic timescale definitions are available, only the determination of the mixing time scale using the geometrical mean definition allows to improve the estimation of the filtered OH formation rate, although affecting the predictions for the other species. The mixing time scale is found to have the highest impact on the predictions of the filtered reaction rates for the investigated cases. The promising results of the PaSR model are obtained for a relatively small filter width, making the model appealing as SGS closure for fine-grid LES. At larger filter widths, the PaSR model loses accuracy, and future work will focus on addressing the sources of modeling bias via data-driven approaches and on validating the PaSR model as a trusted SGS closure for LES of industrial applications of MILD combustion.

Declaration of Competing Interest

The authors declare that they have no known competing financial interests or personal relationships that could have appeared to influence the work reported in this paper.

Acknowledgments

This project has received funding from the European Research Council (ERC) under the European Union's Horizon 2020 research and innovation programme under grant agreement No. 714605. This work used the ARCHER UK National Supercomputing Service (http://www.archer.ac.uk) using computing time provided by EPSRC under the RAP project number e419 and the UKCTRF (e305). S. Iavarone acknowledges the financial support of the Wiener-Anspach Foundation. Z. Chen and N. Swaminathan acknowledge the support of EPSRC. N.A.K. Doan acknowledges the support of the Technical University of Munich - Institute for Advanced Study, funded by the German Excellence Initiative and the European Union Seventh Framework Programme under grant agreement No. 291763.

Supplementary material

Supplementary material associated with this article can be found, in the online version, at doi:10.1016/j.proci.2020.06.234 .

References

[1] International Energy Agency, Key World Energy Statistics (2018). doi:10.1787/key_energ_stat-2018-en.

[2] J.A. Wünning, J.G. Wünning, *Progr. Energy Combust. Sci.* 23 (1) (1997) 81–94, doi:10.1016/S0360-1285(97)00006-3.

[3] A. Cavaliere, M. de Joannon, *Progr. Energy Combust. Sci.* 30 (4) (2004) 329–366, doi:10.1016/j.pecs.2004.02.003.

[4] M. de Joannon, G. Sorrentino, A. Cavaliere, *Combust. Flame* 159 (5) (2012) 1832–1839, doi:10.1016/j.combustflame.2012.01.013.

[5] Y. Minamoto, N. Swaminathan, R.S. Cant, T. Leung, *Combust. Sci. Technol.* 186 (8) (2014) 1075–1096, doi:10.1080/00102202.2014.902814.

[6] N.A.K. Doan, N. Swaminathan, *Combust. Flame* 201 (2019) 234–243, doi:10.1016/j.combustflame.2018.12.025.

[7] A.A.V. Perpignan, A.G. Rao, D.J.E.M. Roekaerts, *Progr. Energy Combust. Sci.* 69 (2018) 28–62, doi:10.1016/j.pecs.2018.06.002.

[8] R. Cabra, J.-Y. Chen, R. Dibble, A. Karpetis, R. Barlow, *Combust. Flame* 143 (4) (2005) 491–506, doi:10.1016/j.combustflame.2005.08.019.

[9] R.L. Gordon, A.R. Masri, S.B. Pope, G.M. Goldin, *Combust. Theory Model.* 11 (3) (2007) 351–376, doi:10.1080/13647830600903472.

[10] A. De, A. Dongre, *Flow Turbul. Combust.* 94 (2) (2015) 439–478, doi:10.1007/s10494-014-9587-8.

[11] F.C. Christo, B.B. Dally, *Combust. Flame* 142 (1) (2005) 117–129, doi:10.1016/j.combustflame.2005.03.002.

[12] E. Oldenhof, M.J. Tummers, E.H. van Veen, D.J.E.M. Roekaerts, *Combust. Flame* 157 (6) (2010) 1167–1178, doi:10.1016/j.combustflame.2010.01.002.

[13] M.J. Evans, P.R. Medwell, Z.F. Tian, *Combust. Sci. Technol.* 187 (7) (2015) 1093–1109, doi:10.1080/00102202.2014.1002836.

[14] C. Duwig, D. Stankovic, L. Fuchs, G. Li, E. Gutmark, *Combust. Sci. Technol.* 180 (2) (2007) 279–295, doi:10.1080/00102200701739164.

[15] M. Ihme, Y.C. See, *Proc. Combust. Inst.* 33 (1) (2011) 1309–1317, doi:10.1016/j.proci.2010.05.019.

[16] J. Chomiak, *Combustion A Study in Theory, Fact and Application*, Abacus Press/Gordon and Breach Science Publishers, New York, 1990.

[17] M. Ferrarotti, Z. Li, A. Parente, *Proc. Combust. Inst.* 37 (4) (2019) 4531–4538, doi:10.1016/j.proci.2018.07.043.

[18] Z. Li, A. Cuoci, A. Parente, *Proc. Combust. Inst.* 37 (4) (2019) 4519–4529, doi:10.1016/j.proci.2018.09.033.

[19] S. Iavarone, M. Cafiero, M. Ferrarotti, F. Contino, A. Parente, *Int. J. Hydrog. Energy* 44 (41) (2019) 23436–23457, doi:10.1016/j.ijhydene.2019.07.019.

[20] B.B. Dally, A.N. Karpetis, R.S. Barlow, *Proc. Combust. Inst.* 29 (1) (2002) 1147–1154, doi:10.1016/S1540-7489(02)80145-6. Proceedings of the Combustion Institute

[21] E. Oldenhof, M.J. Tummers, E.H. van Veen, D.J.E.M. Roekaerts, *Combust. Flame* 158 (8) (2011) 1553–1563, doi:10.1016/j.combustflame.2010.12.018.

[22] Y. Minamoto, N. Swaminathan, *Proc. Combust. Inst.* 35 (3) (2015) 3529–3536, doi:10.1016/j.proci.2014.07.025.

[23] M.U. Göktolga, J.A. Van Oijen, L.P.H. De Goey, *Fuel* 159 (2015) 784–795, doi:10.1016/j.fuel.2015.07.049.

[24] J.A.V. Oijen, *Proc. Combust. Inst.* 34 (1) (2013) 1163–1171, doi:10.1016/j.proci.2012.05.070.
[25] Y. Minamoto, N. Swaminathan, *Combust. Flame* 161 (4) (2014) 1063–1075, doi:10.1016/j.combustflame.2013.10.005.
[26] N.A.K. Doan, N. Swaminathan, Y. Minamoto, *Combust. Flame* 189 (2018) 173–189, doi:10.1016/j.combustflame.2017.10.030.
[27] N. Nordin, *Complex Chemistry Modeling of Diesel Spray Combustion*, Chalmers University of Technology, Chalmers, Sweden, 2001 Ph.D. thesis.
[28] M. Ferrarotti, M. Fürst, E. Cresci, W. De Paepe, A. Parente, *Energy Fuels* 32 (10) (2018) 10228–10241, doi:10.1021/acs.energyfuels.8b01064.
[29] J. Chomiak, A. Karlsson, *Symp. (Int.) Combust.* 26 (2) (1996) 2557–2564, doi:10.1016/S0082-0784(96)80088-9.
[30] R.O. Fox, A. Varma, *Computational Models for Turbulent Reacting Flows*, Cambridge University Press, Cambridge, 2003.
[31] F.P. Kärrholm, *Numerical Modelling of Diesel Spray Injection, Turbulence Interaction and Combustion*, Chalmers University of Technology, Chalmers, Sweden, Ph.D. thesis, 2008.
[32] M. Senouci, A. Bounif, M. Abidat, N.M. Belkaid, C. Mansour, I. Gokalp, *Acta Mech.* 224 (12) (2013) 3111–3124, doi:10.1007/s00707-013-0911-5.
[33] C. Duwig, B. Li, Z. Li, M. Aldén, *Combust. Flame* 159 (1) (2012) 306–316, doi:10.1016/j.combustflame.2011.06.018.
[34] P. Medwell, P. Kalt, B. Dally, *Combust. Flame* 148 (1) (2007) 48–61, doi:10.1016/j.combustflame.2006.10.002.
[35] R.S. Cant, SENGA2 User Guide, CUED/A-THERMO/TR67, Technical report, University of Cambridge, 2013.
[36] M. Valorani, S. Paolucci, P.P. Ciottoli, R.M. Galassi, *Combust. Theory Model.* 21 (1) (2017) 137–157, doi:10.1080/13647830.2016.1243733.